Journal of Physics: Conference Series

PAPER • OPEN ACCESS

Parametric Effects of Fused Deposition Modelling on the Mechanical Properties of Polylactide Composites: A Review

View the article online for updates and enhancements.

Parametric Effects of Fused Deposition Modelling on the Mechanical Properties of Polylactide Composites: A Review

Abraham Kehinde Aworinde[1]*, Samson Oluropo Adeosun[1,2], Festus Adekunle Oyawale[1], Esther Titilayo Akinlabi[1,3], Stephen A. Akinlabi[1,3]

[1] Mechanical Engineering Department, College of Engineering, Covenant University, Ota, Ogun State, Nigeria.
[2] Metallurgical and Material Engineering Department, University of Lagos, Nigeria.
[3] Mechanical Engineering Science Department, University of Johannesburg, South Africa
Corresponding Author: abraham.aworinde@covenantuniversity.edu.ng

Abstract
Polymers are generally inferior in mechanical properties to metals which are the current orthopaedic material for osseointegration in many parts of the world today. This assertion also applies to poly(lactic acid) (PLA), a polyester that has been recently found applicable in tissue remodelling. To improve on its mechanical properties, several processing techniques, inclusive of fused deposition modelling (FDM) also branded as fused filament fabrication (FFF), have been used. FDM has been endeared to many researchers because a range of parameters can be combined to bring about widely different mechanical properties. Although the influence of FDM parameters on the mechanical properties of PLA is clear, the tensile, compressive and flexural strengths obtained so far are inferior to human cortical bone. The need to improve on this production technique for improved mechanical properties is apparent in all the works examined in this review.

Keywords: Additive manufacturing, internal bone fixations, cancellous bone, mechanical properties

1.0   Introduction

Poly(lactic) acid or polylactide (PLA) is an attested biopolymer for medical application [1], especially in soft [2]–[4] and hard [5]–[8] tissue remodelling. It is fast replacing metal and metal alloys in orthopaedics because of some biomechanical issues posed with the use of metal [6], [7], [9]–[15]. In contrast with metals, PLA is biocompatible, biodegradable, bioresorbable and non-carcinogenic [5], [16]–[19]. It, however, has limitations in some applications because of its some degree of hydrophobicity, brittleness and weak mechanical properties.

In a bid to improve on the suitability of PLA for tissue engineering some processing techniques such as solid freeform, fused deposition, rapid prototyping, low-temperature deposition, precise extrusion, indirect solid free form, injection moulding, selective laser sintering, stereolithography, laminated object manufacturing, melt compounding and electrospinning have been used [2], [4], [20]–[30]. This review focuses on Fused Deposition Modelling (FDM). The processing technique in question appears to have a great prospect for the enhancement of the mechanical properties of biodegradable polymers for hard tissue engineering applications while maintaining controlled pores necessary for cell proliferation [31]. Besides, many biodegradable polymer composites have been fabricated via FDM and their properties investigated [32]–[38].

FDM is an additive manufacturing (3D printing process) technology. Unlike subtractive manufacturing, little or no material is wasted. Also, being a computer-aided manufacturing process, the ease with which parameters can be deliberately coordinated makes the manufacturing process better than some other ones like injection moulding, electrospinning, etc. FDM is also advantageous because its maintenance cost is low, the operation is supervision free, materials can be easily changed and the temperature is reasonably low enough to interface with [39]. There is a wide range of parameters that can be controlled to influence the eventual properties of the final product while using FDM.

These parameters include layer thickness, built orientation, raster angle, raster width, air gap, slice height, cusp height, tip diameter [39]–[42], infill density and infill pattern [38], [43]–[48]. To produce parts via fused deposition modelling, a CAD model of the design is created using a CAD software, the model is exported to .stl file, the .stl file is sliced into thin cross-sectional layer to generate G-code, the model is constructed layer by layer on top of each other, while the produced part is then cleaned and made ready for use [40]. The extent to which some of the parameters have affected the mechanical properties of 3D printed PLA and its composites following the outlined FDM process is the focus of this paper.

2.0   Dimensional Accuracy

Generally, it has been observed that FDM parts and CAD models are usually different in dimensions. This difference in dimensions or dimensional error (D_{diff}) between the actual parts and CAD model can be estimated by equation 1 [47].

D_{diff} is a common problem in Additive Manufacturing (AM) of polymers in particular [38], [47], [49]–[51]. D_{diff} will have a significant effect on the mechanical properties of the printed sample if it becomes more pronounced. Its value, for instance, would be higher with FDM parts having high Young's modulus and yield strength, since high dimensional accuracy cannot be achieved if some slicing parameters such as layer thickness and infill density are too high [52]. A high value of D_{diff} would also result if the temperature of the deposited filament is notably higher than the bed or platform temperature.

$$D_{diff} = |D_{CAD} - D_{FDM}| \quad \text{---} \quad (Eq.\ 1)$$

D_{diff} = dimensional difference or dimensional error,

D_{CAD} = dimension of CAD model and

D_{FDM} = dimension of the FDM part or specimen.

D_{diff} has been said to grow with increasing feature size. It was also observed that dimensional difference is always different for holes and bosses under the same printing conditions: the deviation being grater in holes than in bosses of the same model [51]. The fact that growing size increases dimensional error has been established [37] as shown in table 1. The difference between designed and actual pores was seen to be increasing as the designed pore size increases. Slicing parameters, build orientation and temperature conditions concertedly affect compressive, tensile, flexural and other mechanical properties, in varying degrees.

Table 1: Dimensional Differences between Designed and Actual Pore Sizes [37].

Scaffold	D_{CAD} of Pore size (µm)	D_{FDM} of Pore size (µm)	D_{diff} (µm)
Scaffolds type 1	700	726.3 ± 15.0	26.3
Scaffolds type 2	500	522.7 ± 21.6	22.7
Scaffolds type 3	300	318.3 ± 23.2	18.3

3.0   Compressive properties

3D printed materials are generally stronger in compression than in tension [39], [42] and the raster angle has been found to have no significant effect on polymers fabricated by FDM [39]. Specifically, for PLA, varying the infill density (20 to 80%: step of 15%) at constant print speed (75mm/s), layer thickness (0.1mm), shell thickness (1.6mm) and part orientation (90^0), the effect of changing the infill density on the compressive property of PLA was investigated [44]. 3D printed samples were tested according to ASTM D695 standard. Since it has been established that raster angle does not influence the compressive strength of 3D printed parts [39], the effect observed in Figure 1 must, therefore, have been as a result of infill density.

The result (Figure 1) shows that infill density significantly affected the compressive strength and print time. A linear variational relationship was observed between infill density and the output parameters. Higher compressive strength meant higher infill density. More print time would, however, be required as more materials would be deposited. Thus, this can bring about increased D_{diff}. It can be deduced from the result that no material would be deposited at 0% infill density while the maximum amount of material would be deposited at 100%.
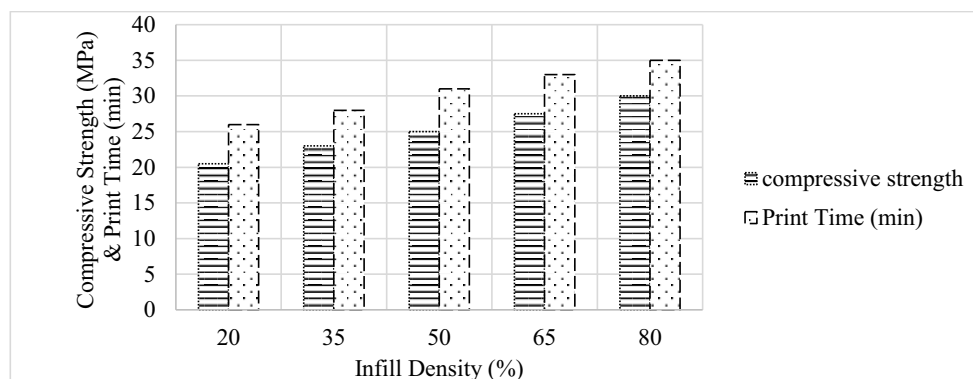

Figure 1: Effect of Infill density on the print time and compressive property of PLA [44].

A porous bar (32 x 86 x 5 mm) with 0.6 mm thick porous layer was fabricated using FDM [53]. Cylinders (Ø10 x 5 mm) were then cut using laser (laser speed = 6.50 mm.s^{-1}, laser power = 12 W) for mechanical behaviour examinations. Raster angle was 0/90^0 while the nozzle diameter, printing temperature and printing speed were respectively 210 ^{0}C, 30 mm.s^{-1} and 0.4 mm. Here the bed temperature which is an important printing parameter in monitoring the dimension of the printed part was not mentioned, neither was infill density parameter quoted.

Compression results showed that yield stress and compressive modulus were slightly different from printed PLA and PLA cut with a laser after printing (Figure 2). The authors observed, however, that values obtained for PLA and laser-cut PLA were both suitable enough to act as replacements for trabecular tissue. In vitro test performed by immersing the samples in

phosphate buffer solution (PBS) also showed an increased value of compressive modulus after 8 weeks of immersion (figure 2).
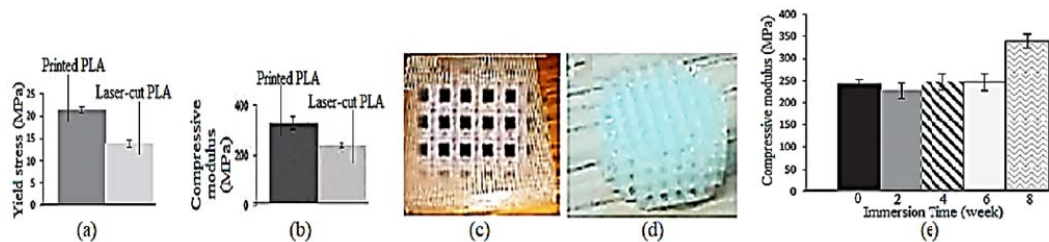

Figure 2: Yield stress (a), Compressive modulus (b) of printed PLA (c) and laser-cut PLA (d) with the compressive modulus of laser-cut PLA after immersion in PBS (e) [53].

The inclusion of controlled pores and pore sizes is one of the amazing possibilities with FDM. Instances where less pore sizes (< 100 μm) than cannot be obtained via FDM were required, gas foaming and solvent etching have been used in conjunction with FDM to create such hierarchical pores. It should be noted that concerted methods of producing hierarchical pores would have a joint effect on the compressive properties, which would be greater than the effect of FDM only. This phenomenon was noticed in the work of Song et al. (2018). Nozzle temperature: 185 ^{0}C, bed temperature: 60 ^{0}C, nozzle diameter: 0.4 mm, printing speed: 45 mm.s^{-1} were the reported parameters used in the FDM production of Poly (vinyl alcohol) (PVA) blended into PLA. Authors did not report the infill density and layer thickness which are the important parameters affecting the eventual mechanical parameters. Pore sizes obtained were, however, stated as shown in Table 1. The compressive moduli of PLA/PVC before and after gas foaming were recorded to be 86.2 ± 13.4 and 17.9 ± 5.2 MPa respectively.

4.0   Parameters affecting Tensile properties

PLA reinforced with carbon nanofiber, CNF was examined for tensile and fracture behaviour by a scholar [38]. 0.4 mm diameter nozzles (circular and square) operating at 230^{0}C, 1.2 mm/s printing speed and deposition plate temperature of 110^{0}C were the fixed printing parameters. During FDM, bed temperature needs to be raised above the ambient to allow for easy removal of the printed parts [37]. Various raster angles were considered in the fabrication of 1%, 0.5% and 0% concentration of CNF in PLA and ASTM D638 followed in the tensile analysis.

It is apparent from the tensile result that square nozzle gave higher values for all the parameters captured in the tensile test. Inter-bead void developed was also lower with square nozzle than with circular nozzle. The values of layer thickness, infill density and infill pattern used were not stated in the work. Infill pattern such as rectilinear, cubic, archiemedeanchords, honeycomb, 3d-honeycomb, octagramspiral, stars, gyroid, etc built into different slicers like Ultimaker Cura, Slic3r, simplify3D, KISSlicer and a host of other slicing software that convert .stl CAD models into G-codes for printing, wield significant impacts on the mechanical properties of 3D printed parts in widely different senses.

The number of shell perimeters has also been found to affect the tensile property of PLA [46]. Keeping the nozzle diameter (0.50 mm), layer height, printing speed and outline overlap constant, PLA was printed in conformity to ASTM D638-14 for mechanical tensile property examination with each sample having either 1 perimeter shell or 3 perimeter shells. Results

showed that variations in infill density (15, 30 and 50%) and infill pattern (hexagonal, triangular, square, square diagonal, reinforced square diagonal) notwithstanding (Figure 3), all samples with 3 perimeter shells had higher tensile property.
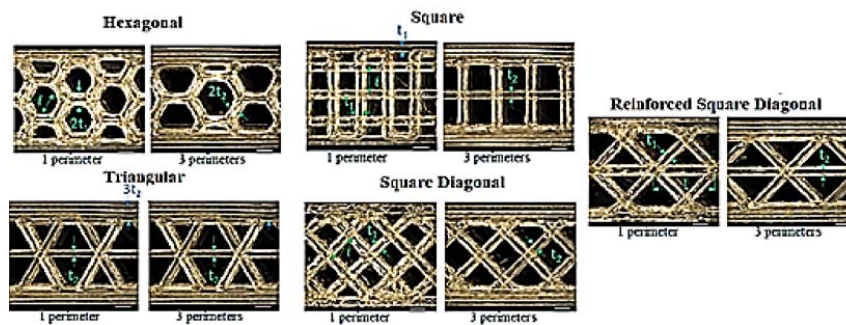

Figure 3: Optical microscopy images of various infill patterns printed with 1 and 3 perimeter shells [46].

Layer height and raster angle were discovered to be grave parameters in determining tensile strength [54]. Samples fabricated at 100 µm layer height and 0^0 raster angle were found to have the highest tensile strength. The examined layer heights were 100, 200 and 300 µm. It appears that the smaller the layer height, the higher the tensile strength, possibly until a threshold is reached. 0^0 raster angle reduces the sample anisotropy. High tensile strength, therefore, results as the sample is pulled longitudinally along raster angle orientation.

5.0   Parameters affecting Flexural properties

Raster angle, the angle between the printing nozzle and the printing bed, and raster width reportedly affect the mechanical flexural strength of FDM parts significantly [54]. With the printing temperature (210 ^{0}C), bed temperature (70 ^{0}C), printing speed (50 mm.s^{-1}), number of perimeters (1), infill density (100%), infill pattern (rectilinear) being fixed, raster angle (0, 45, 90 ^{0}C), layer height (100, 200, 300 µm) and raster width (500, 600, 700 µm) were varied between three values each.

Of all samples printed at 500 µm raster width, the one printed at 45^0 raster angle and 100 µm layer height had the highest flexural strength. The flexural strength value (~77.5 MPa) obtained at these printing parameters was about the same magnitude with the values obtained for FDM parts printed at 600 µm raster width, 45^0 raster angle and 100 µm layer height. Again, approximately the same value was recorded when the printing parameters were 700 µm raster width, 0^0 raster angle and 200 µm layer height. Similarly, raster angle/raster width/layer height combination that gave ~77.5 MPa were 0^0/700 µm/200 µm, 45^0/500 µm /100 µm and 90^0/600 µm/100 µm.

Deductively, lower layer height and 45^0 raster angles would give higher flexural strength. For larger raster width, it is advisable to print at 0^0 raster angle. It has also been established that layer thickness affects the flexural properties [55]

6.0   General mechanical Properties

Taguchi method was explored to study the effect of the layer thickness, infill density, extrusion temperature and infill pattern on the properties of PLA [47]. Dimensional accuracy, the strength

of printed parts and ductility were found to be mutually exclusive: combining the input parameters in various ways gives widely different outputs (Table 2).

Table 2: Optimal FDM parameters for various mechanical properties [47], [54]

Required output	Input parameters			
	Infill density (%)	Infill pattern	Extrusion temperature (^{0}C)	Layer thickness (mm)
Dimensional accuracy	20	hexagonal	190	0.2
Tensile strength (MPa)	100	triangular	210	0.3
Ductility (%)	20	rectilinear	200	0.4
E (MPa)	100	rectilinear	210	0.3
Yield strength (MPa)	100	triangular	200	0.4
Flexural strength (MPa)	100	*rectilinear	210	0.1

*some works did not use rectilinear infill pattern to obtain optimal flexural strength.

Conclusions

FDM is a versatile polymer production technique. The range of parameters which can be combined to bring about various mechanical properties is vast. However, the mechanical properties of PLA samples produced via FDM are still lower than the mechanical properties of the human cortical bone. While the PLA FDM produced samples can fitly help trabeculae, there is a need to research more into a combination of parameters that will give printed PLA unusual mechanical properties comparable to the human cortical bone for proper osteosynthesis.

Reinforcement of PLA with biodegradable polymer-particles (e.g chitosan and chitin) and ceramic-particles (e.g hydroxyapatite) to produce filaments has not been pronounced. Apart from the enhancement of biodegradation which can be the result of such composite filaments, there are possibilities that the mechanical properties would also be enhanced.

Compressive properties would be expected to be greater than tensile properties for FDM with organised pores. This holds as compressive load collapses some pores with the passage of time, making the material to become stiffer and leading to increasing modulus before the commencement of biodegradation. The possibility of fabricating interconnected pores makes the production of PLA by FDM a *sine qua non* in the production of implants that allow for cell proliferation and differentiation.

Acknowledgements

REFERENCE

[1]   B. Tyler, D. Gullotti, A. Mangraviti, T. Utsuki, and H. Brem, "Polylactic acid (PLA) controlled delivery carriers for biomedical applications ☆," *Adv. Drug Deliv. Rev.*, vol.

107, pp. 163–175, 2016.

[2]   S. Deepthi, M. Nivedhitha Sundaram, J. Deepti Kadavan, and R. Jayakumar, "Layered chitosan-collagen hydrogel/aligned PLLA nanofiber construct for flexor tendon regeneration," *Carbohydr. Polym.*, 2016.

[3]   S. O. Adeosun, A. K. Aworinde, I. V Diwe, and S. A. Olaleye, "Mechanical and Microstructural Characteristics of Rice Husk Reinforced Polylactide Nano Composite," *West Indian J. Eng.*, vol. 39, no. 1, pp. 63–71, 2016.

[4]   O. P. Gbenebor, R. A. Atoba, E. I. Akpan, A. K. Aworinde, S. O. Adeosun, and S. A. Olaleye, "Study on Polylactide-Coconut Fibre for Biomedical Applications," in *TMS 2018 147th Annual Meeting & Exhibition Supplemental Proceedings*, M. & Materials Society, The Minerals, Ed. Cham: Springer International Publishing, 2018, pp. 263–273.

[5]   Z. Wang, Y. Wang, Y. Ito, P. Zhang, and X. Chen, "A comparative study on the in vivo degradation of poly(L-lactide) based composite implants for bone fracture fixation," *Sci. Rep.*, vol. 6, pp. 1–12, 2016.

[6]   A. K. Aworinde, S. O. Adeosun, F. A. Oyawale, E. T. Akinlabi, and E. Emagbetere, "Mechanical Strength and Biocompatibility Properties of Materials for Bone Internal Fixation : A Brief Overview," in *Proceedings of the International Conference on Industrial Engineering and Operations Management*, 2018, pp. 1–12.

[7]   F. Ya'ish, C. A. Bailey, C. P. Kelly, and M. A. Craigen, "Bioabsorbable Fixation of Scaphoid Fractures and Non-Unions; Analysis of Early Clinical Outcomes," *Hand Surg.*, vol. 18, no. 03, pp. 343–349, 2013.

[8]   R. Mittal, J. Morley, H. Dinopoulos, E. G. Drakoulakis, E. Vermani, and P. V. Giannoudis, "Use of bio-resorbable implants for stabilisation of distal radius fractures: The United Kingdom patients' perspective," *Injury*, vol. 36, no. 2, pp. 333–338, 2005.

[9]   B. V. & B. S. Orringer J., "Reasons for removal of rigid internal fixation devices in craniofacial surgery," *J. Craniofac Surg.*, vol. 9, pp. 40–4, 1998.

[10] M. D. Michael J Yaremchuk, M.D., Thomas G.S. Fiala, M.D., Frederick Barker, M.D., and Ronald Ragland, "The effects of rigid fixation on craniofacial growth of rhesus monkeys," *Plast Reconstr Surg*, vol. 93, pp. 1–10, 1994.

[11] A. U. Daniels, M. K. O. Chang, K. P. Andriano, and J. Heller, "Mechanical properties of biodegradable polymers and composites proposed for internal fixation of bone," *J. Appl. Biomater.*, vol. 1, no. 1, pp. 57–78, 1990.

[12] P. N. M. Daniel S. Jorgenson, Micheal H. Mayer, Richard G. Ellenbogen, Jose A. Centeno, Frank B. Johnson, Florabel G. Mullick, "Detection of Titanium in Human Tissues after Craniofacial Surgery," *Plast. Reconstr. Surg.*, vol. 99, no. 4, pp. 976–979, 1997.

[13] J. J. Dias, "Definition of Union after Acute Fracture and Surgery for Fracture Nonunion of the Scaphoid." pp. 321–325, 2001.

[14] F. Katou, N. Andoh, K. Motegi, and H. Nagura, "Immuno-inflammatory responses in the tissue adjacent to titanium miniplates used in the treatment of mandibular fractures," *J. Cranio-Maxillo-Facial Surg.*, vol. 24, pp. 155–162, 1996.

[15]   P. A. Steven R. Cohen, Ralph E. Holmes and H. F. and E. M. Shusterman, "Technical Strategies Tacks: A New Technique for Craniofacial Fixation," *J. Craniofac Surg.*, vol. 12, no. 6, pp. 596–602, 2001.

[16]   P. A. Gunatillake, R. Adhikari, and N. Gadegaard, "Biodegradable synthetic polymers for tissue engineering," *Eur. Cells Mater.*, vol. 5, pp. 1–16, 2003.

[17]   J. C. Middleton and A. J. Tipton, "Synthetic biodegradable polymers as orthopedic devices," *Biomaterials*, vol. 21, no. 23, pp. 2335–2346, 2000.

[18]   L. Xiao, B. Wang, G. Yang, and M. Gauthier, "Poly(Lactic Acid)-Based Biomaterials: Synthesis, Modification and Applications." pp. 247–282, 2012.

[19]   S. Kakinoki, S. Uchida, T. Ehashi, A. Murakami, and T. Yamaoka, "Surface modification of poly(l-lactic acid) nanofiber with oligo(D-lactic acid) bioactive-peptide conjugates for peripheral nerve regeneration," *Polymers (Basel).*, vol. 3, no. 2, pp. 820–832, 2011.

[20]   Z. Xiong, Y. Yan, S. Wang, R. Zhang, and C. Zhang, "Fabrication of porous scaffolds for bone tissue engineering via low-temperature deposition," *Scr. Mater.*, vol. 46, no. 11, pp. 771–776, 2002.

[21]   Z. Xiong, Y. Yan, R. Zhang, and L. Sun, "Fabrication of porous poly (L -lactic acid) sca   olds for bone tissue engineering via precise extrusion," *Acta Mater.*, vol. 45, pp. 773–779, 2001.

[22]   S. O. Adeosun, A. K. Aworinde, I. V. Diwe, and S. A. Olaleye, "Mechanical and Microstructural Characteristics of Rice Husk Reinforced Polylactide Nanocomposite," *West Indian J. Eng.*, vol. 39, no. 2, pp. 63–71, 2016.

[23]   M. S. Abu Bakar, P. Chenag, and K. A. Khor, "Mechanical properties of injection molded hydroxyapatite-polyetheretherketone biocomposites," *Compos. Sci. Technol.*, vol. 63, no. 3–4, pp. 421–425, 2003.

[24]   M. Aslam, F. Ahmad, P. S. M. B. M. Yusoff, K. Altaf, M. A. Omar, and R. M. German, "Powder injection molding of biocompatible stainless steel biodevices," *Powder Technol.*, vol. 295, pp. 84–95, 2016.

[25]   D. W. Hutmacher, T. Schantz, I. Zein, K. W. Ng, S. H. Teoh, and K. C. Tan, "Mechanical properties and cell cultural response of polycaprolactone scaffolds designed and fabricated via fused deposition modeling," no. 4, 2001.

[26]   U. Jammalamadaka and K. Tappa, "Recent Advances in Biomaterials for 3D Printing and Tissue Engineering," *J. Funct. Biomater.*, vol. 9, no. 1, p. 22, 2018.

[27]   F. M. Michael *et al.*, "Effect of nanofillers on the physico-mechanical properties of load bearing bone implants," *Mater. Sci. Eng. C*, vol. 67, pp. 792–806, 2016.

[28]   M. J. Mondrinos *et al.*, "Porogen-based solid freeform fabrication of polycaprolactone-calcium phosphate scaffolds for tissue engineering," *Biomaterials*, vol. 27, no. 25, pp. 4399–4408, 2006.

[29]   J. M. Taboas, R. D. Maddox, P. H. Krebsbach, and S. J. Hollister, "Indirect solid free form fabrication of local and global porous, biomimetic and composite 3D polymer-ceramic scaffolds," *Biomaterials*, vol. 24, no. 1, pp. 181–194, 2003.

[30] R. C. Thomson, M. J. Yaszemski, J. M. Powers, and A. G. Mikos, "Fabrication of biodegradable polymer scaffolds to engineer trabecular bone," *J. Biomater. Sci. Polym. Ed.*, vol. 7, no. 1, pp. 23–38, 1995.

[31] S. Jyoti, S. Bose, H. L. Hosick, and A. Bandyopadhyay, "Development of controlled porosity polymer-ceramic composite scaffolds via fused deposition modeling," vol. 23, pp. 611–620, 2003.

[32] X. Wang, M. Jiang, Z. Zhou, J. Gou, and D. Hui, "3D printing of polymer matrix composites: A review and prospective," *Compos. Part B Eng.*, vol. 110, pp. 442–458, 2017.

[33] F. Daver, K. P. M. Lee, M. Brandt, and R. Shanks, "Cork–PLA composite filaments for fused deposition modelling," *Compos. Sci. Technol.*, vol. 168, no. September, pp. 230–237, 2018.

[34] C. Esposito Corcione *et al.*, "Highly loaded hydroxyapatite microsphere/ PLA porous scaffolds obtained by fused deposition modelling," *Ceram. Int.*, no. xxxx, pp. 1–8, 2018.

[35] G. Chen, N. Chen, and Q. Wang, "Preparation of poly (vinyl alcohol)/ionic liquid composites with improved processability and electrical conductivity for fused deposition modeling," *Mater. Des.*, vol. 157, pp. 273–283, 2018.

[36] M. Sabino *et al.*, *In vitro biocompatibility study of biodegradable polyester scaffolds constructed using fused deposition modeling (FDM)*, vol. 6, no. PART 1. IFAC, 2013.

[37] P. Song *et al.*, "Novel 3D porous biocomposite scaffolds fabricated by fused deposition modeling and gas foaming combined technology," *Compos. Part B Eng.*, vol. 152, no. June, pp. 151–159, 2018.

[38] E. A. Papon and A. Haque, "Tensile properties, void contents, dispersion and fracture behaviour of 3D printed carbon nanofiber reinforced composites," *J. Reinf. Plast. Compos.*, vol. 37, no. 6, pp. 381–395, 2018.

[39] W. Wenzheng, G. Peng, L. Guiwei, Z. Di, Z. Haibo, and Z. Ji, "Influence of layer thickness and raster angle on the mechanical properties of 3D-printed PEEK and a comparative mechanical study between PEEK and ABS," *Materials (Basel).*, vol. 8, no. 9, pp. 5834–5846, 2015.

[40] R. Singh and H. K. Garg, "Fused Deposition Modeling – A State of Art Review and Future Applications," 2016.

[41] D. Popescu, A. Zapciu, C. Amza, F. Baciu, and R. Marinescu, "FDM process parameters influence over the mechanical properties of polymer specimens: A review," *Polym. Test.*, vol. 69, no. April, pp. 157–166, 2018.

[42] J. R. C. Dizon, A. H. Espera, Q. Chen, and R. C. Advincula, "Mechanical characterization of 3D-printed polymers," *Addit. Manuf.*, vol. 20, pp. 44–67, 2018.

[43] M. Fernandez-Vicente, W. Calle, S. Ferrandiz, and A. Conejero, "Effect of Infill Parameters on Tensile Mechanical Behavior in Desktop 3D Printing," *3D Print. Addit. Manuf.*, vol. 3, no. 3, pp. 183–192, 2016.

[44] T. Abbas, F. M. Othman, and H. B. Ali, "Effect of infill Parameter on compression property in FDM Process," *Int. J. Eng. Res. andApplication*, vol. 7, no. 10, pp. 16–19,

2017.

[45] R. Ricotti *et al.*, "Dosimetric characterization of 3D printed bolus at different infill percentage for external photon beam radiotherapy," *Phys. Medica*, vol. 39, pp. 25–32, 2017.

[46] C. Lubombo and M. A. Huneault, "Effect of infill patterns on the mechanical performance of lightweight 3D-printed cellular PLA parts," *Mater. Today Commun.*, vol. 17, no. September, pp. 214–228, 2018.

[47] A. Alafaghani and A. Qattawi, "Investigating the effect of fused deposition modeling processing parameters using Taguchi design of experiment method," *J. Manuf. Process.*, vol. 36, no. September, pp. 164–174, 2018.

[48] J. Wu, A. Clausen, and O. Sigmund, "Minimum compliance topology optimization of shell–infill composites for additive manufacturing," *Comput. Methods Appl. Mech. Eng.*, vol. 326, pp. 358–375, 2017.

[49] E. Yankov and M. P. Nikolova, "Comparison of the Accuracy of 3D Printed Prototypes Using the Stereolithography (SLA) Method with the Digital CAD Models," *MATEC Web Conf.*, vol. 137, p. 02014, 2017.

[50] A. Reyes-Rodríguez, R. Dorado-Vicente, and R. Mayor-Vicario, "Dimensional and form errors of PC parts printed via Fused Deposition Modelling," *Procedia Manuf.*, vol. 13, pp. 880–887, 2017.

[51] S. Mahmood, A. J. Qureshi, and D. Talamona, "Taguchi based process optimization for dimension and tolerance control for fused deposition modelling," *Addit. Manuf.*, vol. 21, no. March, pp. 183–190, 2018.

[52] A. Lanzotti, M. Grasso, G. Staiano, and M. Martorelli, "The impact of process parameters on mechanical properties of parts fabricated in PLA with an open-source 3-D printer," *Rapid Prototyp. J.*, vol. 21, no. 5, pp. 604–617, 2015.

[53] N. Rodrigues, M. Benning, A. M. Ferreira, L. Dixon, and K. Dalgarno, "Manufacture and Characterisation of Porous PLA Scaffolds," *Procedia CIRP*, vol. 49, pp. 33–38, 2016.

[54] S. R. Rajpurohit and H. K. Dave, "Flexural strength of fused filament fabricated (FFF) PLA parts on an open-source 3D printer," 2018.

[55] A. Nugroho, R. Ardiansyah, L. Rusita, and I. L. Larasati, "Effect of layer thickness on flexural properties of PLA (PolyLactid Acid) by 3D printing," *J. Phys. Conf. Ser.*, vol. 1130, no. 1, 2018.